Energy for Sustainable Development 32 (2016) 130–139

Contents lists available at ScienceDirect

Energy for Sustainable Development

Characterization of gaseous and particulate pollutants from gasification-based improved cookstoves

Sameer Patel, Anna Leavey, Siqin He [1], Jiaxi Fang, Kyle O'Malley, Pratim Biswas *

Aerosol and Air Quality Research Laboratory, Department of Energy, Environmental and Chemical Engineering, Washington University in St. Louis, St. Louis, MO 63130, USA

ARTICLE INFO

Article history:
Received 19 August 2015
Revised 8 February 2016
Accepted 8 February 2016

ABSTRACT

Cookstove studies have reported pollutant concentrations (mainly $PM_{2.5}$, black carbon and CO) without routinely associating it with the design and operating principles of the stoves. Extensive characterization of pollutants from cookstoves and the effect of different operating conditions are required for a better understanding of the mechanisms of pollutant formation. In this study, a forced draft (FD) and a natural draft (ND) gasification-based improved cookstove were tested under controlled conditions. Real-time pollutant concentrations, both particulate ($PM_{2.5}$, lung-deposited surface area and particle number size distribution) and gaseous (CO, CO_2 and NO_x), from these stoves using three types of fuel (applewood chips and chunks, cowdung cake and coal) along with different cookstove operating conditions (airflow rates and with or without a cooking pot) were measured and compared. The FD cookstove tended to exhibit higher concentrations of emissions compared to the ND cookstove. Increasing airflow through the FD stove decreased flame length and the residence time of VOCs inside the flame zone, which in turn increased pollutant concentrations. An optimum airflow producing the lowest particulate matter (PM) concentrations was established for the FD cookstove. The CO–CO_2 ratio, an indicator of combustion efficiency, demonstrated strong correlations with $PM_{2.5}$ ($r = 0.857$), particle geometric mean diameter ($r = 0.900$) and the total surface area concentration ($r = 0.908$) indicating that CO–CO_2 ratio may be used as a proxy for these PM metrics. Results reported in this study will facilitate further improvements in the design of future cookstoves.

Introduction

Two million tons of biomass, including animal dung and agricultural residue, are burned daily in cookstoves in the developing world (Naeher et al., 2007), and along with coal, provides energy for space heating and cooking to almost three billion of the world's poorest people (Rehfuess, 2006). High concentrations of pollutants such as particulate matter (PM), carbon monoxide (CO) and organic compounds are emitted due to incomplete combustion of these solid fuels in cookstoves. Inhaled ultrafine particles (UFP) generated from solid fuel combustion can evade the body's mucocilliary defense system and deposit deep in the alveolar region of the lungs leading to short-term inflammation and oxidative stress (Naeher et al., 2007), and long-term chronic obstructive pulmonary disorders (COPD) (Smith, 2002). Other diseases from exposure to biomass emissions include acute respiratory infections (ARI), cataracts and tuberculosis (Smith, 2002; Bruce et al., 2000). The World Health Organization reported that the exposure to air pollution led to 7 million deaths in 2012, making it the world's largest single environmental health risk (Global Health Observatory). Household air pollution accounted for more than half of these deaths.

The majority of those who rely on solid fuels use traditional three-stone cookstoves and open fires to cook their food (Legros, 2009). Studies have reported concentrations exceeding 10 mg/m^3 and 300 ppm for $PM_{2.5}$ and CO, respectively (Chengappa et al., 2007; Sahu et al., 2011; Roden et al., 2006; Leavey et al., 2015). Because most of the improved cookstoves have better combustion efficiency, they produce fewer emissions, thus renewed impetus to promote and distribute these cookstoves has seen the number of people using them rise to approximately 800 million (Legros, 2009; Anon., 2011). However, combustion efficiency differs widely between these improved cookstoves with gasification-based cookstove among the best performing stoves. Laboratory studies comparing both the forced-draft (FD) and less frequently the natural-draft (ND) gasification-based stove, to other cookstoves have repeatedly demonstrated their improved efficiency and reduced emissions (Kar et al., 2012; MacCarty et al., 2008; Jetter & Kariher, 2009; Jetter et al., 2012). For example, Kar et al. (2012) reported a 77% reduction in black carbon (BC) emissions for the FD Philips stove compared to a traditional mud cookstove, while Jetter et al. (2012) reported lower CO and $PM_{2.5}$ emissions per unit energy delivered to the cooking pot compared

* Corresponding author. Tel.: +1 314 935 5548; fax: +1 314 935 5464.
E-mail addresses: sameer@wustl.edu (S. Patel), aleavey@seas.wustl.edu (A. Leavey), siqin.he@kanomaxfmt.com (S. He), jiaxi@wustl.edu (J. Fang), komalley@wustl.edu (K. O'Malley), pbiswas@wustl.edu (P. Biswas).
[1] Present affiliation: Kanomax FMT Inc., 4106 Hoffman Road, White Bear Lake, MN 55110, USA.

http://dx.doi.org/10.1016/j.esd.2016.02.005
0973-0826/

to a three-stone stove. With the exception of a few studies (Jetter & Kariher, 2009; MacCarty et al., 2010), correlating pollutant concentrations with the design and operating principles of a particular cookstove has rarely been done. Such correlations are critical for further improvements to cookstove design.

Another important aspect is a protocol for testing the stove which will allow comparisons. Many researchers have proposed a Water Boiling Test (WBT). However, this test has limitations which are defined in the WBT protocol itself (Water Boiling Test Protocol). The WBT does not prescribe the exact pot to be used for the tests. This introduces another variable (size and material of the pot) potentially changing the emission characteristics. L'Orange et al. (2012) showed that the pot temperature has a significant effect on PM characteristics. For example, a hot pot resulted in lower PM_{10} with lower smaller particle sizes. Other tests, such as the Controlled Cooking Test (CCT) and Uncontrolled Cooking Test (UCT) better capture cookstove performance when cooking actual food in both laboratory and field settings. Arora et al. (2014) followed the CCT to demonstrate that emissions characteristics depend on the type of meal cooked, and not just the type of meal but even the thickness of a roti (a type of Indian bread) altered emissions. They found CO fluctuated by up to 49% depending on different cooking styles. Because recently published studies are increasingly demonstrating the effect that small changes in cooking (pot/food/water temperature) alter emission characteristics, it is clear that the WBT and other similar laboratory tests fail to represent field conditions. Although it is true that cookstoves are rarely used without a pot, their performance in the absence of a pot must be investigated to gain a fundamental understanding of the combustion processes to avoid complexity and reduce uncertainty especially in controlled laboratory studies. Such combustion studies are often lacking due to the emphasis of establishing emission factors (EF) which vary significantly based on the field cooking styles, and therefore do not accurately correspond to eventual health or climate impacts.

Although Jetter and Kariher (2009) compared cookstove performance for different types of biomass, few studies have incorporated dung and coal into their analysis, a key gap given that: (1) dung features low on the energy ladder and is therefore used by the poorest and most vulnerable members of society (Rehfuess, 2006; Pohekar et al., 2005); and (2) coal continues to dominate in certain communities and is especially heinous. For example, in the Damodar Valley, India, 2.55 million tons of coal are consumed domestically each year (Erkman & Ramaswamy, 2003). Households that burn coal consistently demonstrate higher pollutant concentrations compared to those that burn biomass (Zhang & Smith, 2007). Impaired immune system, CO poisoning, COPD and lung cancer have been reported from exposure to coal combustion emissions (Naeher et al., 2007; Zhang & Smith, 2007). Finally, with the exception of a handful of studies that have incorporated multiple particulate metrics, including particle number size distributions, into their study (Armendáriz-Arnez et al., 2010; Zhang et al., 2012; Fang et al., 2014; Just et al., 2013; Shen et al., 2011), most studies focus on $PM_{2.5}$ and CO. Also, with the exception of a couple of studies (Sahu et al., 2011; Leavey et al., 2015), lung-deposited surface area has not been investigated.

The overall objective of this study was to conduct an extensive characterization of particulate and gaseous pollutants from biomass and coal burned in two gasification-based improved cookstoves; FD Philips (HD 4012) stove and ND Quad, a Top Lit Updraft (TLUD) stove. Correlations between concentrations of different pollutants were investigated to evaluate the feasibility of using one pollutant as a proxy for others. In addition, the influence of a cooking pot on pollutant concentrations was assessed. Finally, the Philips stove was operated at 3 different airflows to examine the influence on particle number size distribution (PNSD). Results obtained in this study were explained based on the operating principles of gasification-based cookstoves. Comparisons between the FD and ND stoves enhanced the understanding of pollutant formation which should facilitate further improvements in design of the stoves.

Materials and methods

Different system components are described in the following sections. An overall test plan is provided in Table 1.

Cookstoves studied

Two gasification-based cookstoves, the Philips (Model No. HD4012 LS) and the Quad TLUD were investigated. As illustrated in Fig. 1, primary air passes through the inner cylinder, where the biomass is placed. Biomass gasification occurs in the primary oxidation zone (lower region) in the presence of limited oxygen. Producer gas, consisting mainly of CO, lower hydrocarbons and volatiles, is then oxidized by the air in the secondary oxidation zone at the top of the cookstove. A more detailed description of design and operating principles of the stoves is discussed in the following section: construction and operating principle of the gasification-based cookstoves.

Fuels

The three fuels investigated were applewood, cowdung cake and coal. Each of these fuels are used by different income groups. Cowdung cake is a popular fuel in rural India, especially among households with low and medium income (Pohekar et al., 2005). Fresh dung from grass-fed cows was collected from a farm near St. Louis (Missouri), shaped into patties and left to dry in the open for two weeks during the summer season. Chemically untreated applewood was purchased locally. Two sizes of applewood, chips (1–3-cm-long thin pieces) and chunks (4–6 cm cubes), were tested to examine the effect of fuel size. Bituminous coal from Brilliant (Alabama) was also tested. Fuels were procured from the same batch and stored at constant ambient conditions to minimize variability. The properties of the various fuels used are reported in the literature and vary from reference to reference: proximate analysis, ultimate analysis and heating value for applewood (Fang et al., 2014; Yang et al., 2014; Verma et al., 2012), dung cakes (Venkataraman & Rao, 2001; Singh et al., 2013; Kandpal & Maheshwari, 1995) and bituminous coal (Bond et al., 2002; McKendry, 2002).

Experimental setup

Experiments were conducted in a fume hood in a controlled environment to facilitate comparisons by minimizing the variability between different runs. A schematic diagram of the experimental setup is shown in Fig. 2. A hood with a 0.37 m^2 area was installed above the cookstove. Flow from the hood was sampled using an aspiration-based sampling system (Ahn et al., 2001; Biswas, 2001). The aspiration-based sampling system creates a suction using low pressure generated from the flow of dilution air; therefore, no pump downstream is required. A dilution flow of 0.094 cubic meters per minute was used to achieve a dilution ratio of 4. After the dilution unit, a fraction of the sample was collected by an isokinetic sampling probe while the rest was vented out. The sample then passed through a diffusion dryer to remove any moisture to prevent interference with readings. Copper and conductive tubing was used throughout the sampling train to minimize particle loss during transport.

The test plan for this study is outlined in Table 1. Unlike the water boiling test (WBT), which assesses thermal efficiency (Jetter & Kariher, 2009; Jetter et al., 2012) under controlled settings, this work focused on the pollutant characteristics (concentrations and size distribution in case of PM) as a result of the gasification/combustion processes in different cookstoves. All tests were done without a cooking pot as the focus was on the gasification-combustion process. However, one test (ID 9, Table 1) was performed with a pot to examine its influence and also

Table 1
Experimental plan for laboratory test of cookstoves.

Test ID	Cookstove	Fuel type	Fuel load (g)	Air flow	Objective
1	Philips	Applewood chips	210	Medium	Fuel comparison
2		Applewood chunks	280		
3		Cowdung cake	110		
4		Coal	650		
5	TLUD	Applewood chips	860		Fuel comparison
6		Applewood chunks	1200		
7		Cowdung cake	450	NA	Stove comparison
8		Coal	2500		
9		Applewood chips (with pot)	860		Impact of pot
10	Philips	Applewood chips	210	Low	Impact of airflow (with Test 1)
11		Applewood chips	210	High	

to highlight that a pot is an important variable that impacts emissions. The TLUD stove was fired using applewood chips and a pot with 5 L of water. The quantity of water was selected to ensure that it hovered just below the boiling point, thus minimizing any interference with instrument readings from added moisture. The impact on emissions on use of a pot is, however, more complex (e.g. size, shape and material of the pot) and was not in the scope of this study. The Philips stove, fueled with applewood chips, was tested at three different airflow rates: low, medium and high, to assess its effect on particulate emissions. Each experimental test was repeated a minimum of three times. Observations on the flame structure (length and intensity) and smoke characteristics were also noted.

Characterization of particulate and gaseous pollutants

Total number concentrations and PNSD were measured using a scanning mobility particle sizer (SMPS 3080, TSI) and a condensation particle counter (CPC 3022, TSI). The SMPS operates by charging particles to a known charge distribution by a bipolar charger in an electrostatic classifier. Charged particles are then classified based on their electrical mobility in an electric field and an optical sensor in the CPC measures the number concentration. Real-time measurements of lung-deposited surface area were made using a nanoparticle surface area monitor (AeroTrak 9000, TSI). This instrument can provide surface area concentrations of particles deposited in either the tracheobronchial (TB) or alveolar (A) regions of the lung based on deposition curves obtained from models developed by the International Commission on Radiological Protection (ICRP) (Bailey, 1994). The surface area concentration of particles deposited in the TB region was recorded in this study. Details about the operating principles of the AeroTrak 9000 are provided in Leavey et al. (2013).

A DustTrak II (Model 8532, TSI) was used to monitor $PM_{2.5}$. This portable instrument works on the principle of light scattering. A fraction of the sample flow, to be used as sheath flow, is passed through a HEPA filter. Particles scatter the light, as they pass a laser diode. The degree of light scattering depends on the size, shape and density of the particles. The scattered light falls on a spherical mirror which focuses it on a photo detector resulting in a voltage which is proportional to mass concentration.

The EL-USB-CO EasyLog®, manufactured by LASCAR Electronics, was used to record CO levels. It oxidizes CO to CO_2 producing a current proportional to the CO concentration. The range of the instrument is 0–300 ppm with the smallest data logging interval of 10 seconds. A portable gas analyzer (HORIBA PG-250) was used to measure CO_2 and NO_x levels. The NO_x unit uses a cross-flow modulation chemiluminescence, while the CO_2 unit operates on the principle of the non-dispersive infrared (NDIR) method. A LabVIEW® program was created for data acquisition, and so that data could be stored in one-second intervals.

Analysis

The burn cycle of the stoves was divided into three phases: the ignition, steady-state and extinguishing phase (Fig. 3). This study focused on data collected while the cookstove was operating under steady-state burning conditions, as this represents the major part of the total operation time and is the phase during which cooking occurs. The steady-state phase was defined as the time period during which concentrations of CO and CO_2 were relatively stable, and a flame with constant intensity and length was observed. The ignition phase was marked as the time between the ignition and start of the steady-state phase. Similarly, the extinguishing phase was marked from end of the steady-state phase until flame extinction. The duration of steady-state varies with stove, fuel type and experimental settings. In a field study, Sahu et al. (2011) reported the start of steady-state at approximately 20 min post-ignition, while Leavey et al. (2015) reported an interval of 2–15 min between ignition and the start of steady-state phase in an another field study. In this laboratory study, steady-state began within

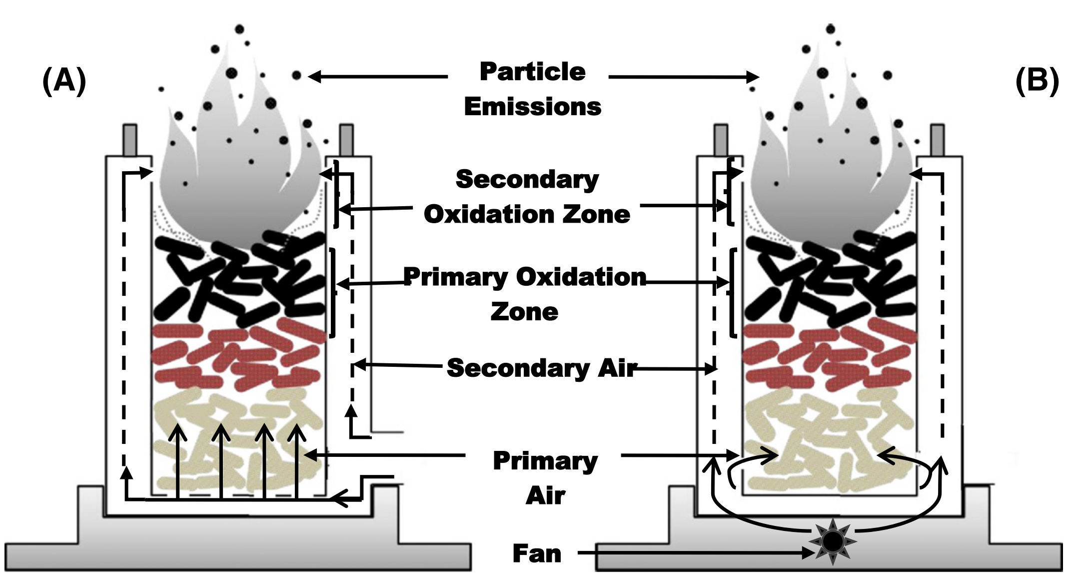

Fig. 1. Schematic diagram of (A) the natural draft top-lit updraft (TLUD) and (B) the forced draft Philips™ stove.

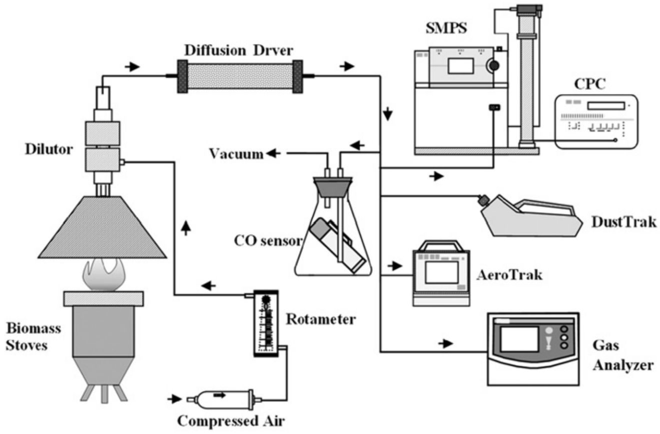

Fig. 2. Experimental setup for real-time emission characterization.

2–5 min from ignition, depending on stove and fuel type. A plausible explanation for this disparity is the optimal conditions under which experiments were conducted in the laboratory and the difference in the type of cookstoves used. In the case of coal, two steady-states were defined, the flame phase characterized by flames and heavy smoke and the smoldering phase when the flames have died out leaving only red-hot glowing coal. The duration and the heat generation rate of both phases were found to be comparable but pollutant characteristics during these two phases differed significantly.

This study reports average concentrations over the steady-state phase only. While most of the PM metrics measured directly, mass and surface area concentrations were calculated using PNSD data from the SMPS. To analyze the correlation between concentrations of different pollutants, a correlation test was performed using R Statistical Software (version 2.101).

Construction and operating principle of the gasification-based cookstoves

The typical construction of a gasification-based cookstove includes two concentric cylinders open at each end (Fig. 1). Design parameters of the two stoves are presented in Table 2. Fuel is placed in the inner cylinder and air flowing through it is labelled as the primary airflow. The annular region between the two cylinders acts as a channel for the secondary airflow. Unlike a fan installed at the bottom of FD cookstoves, a temperature gradient along the height of the stove creates an updraft in ND cookstoves. Thus, ND cookstoves are generally taller than FD cookstoves to create a comparable updraft. Also, as most of the FD cookstoves require a power source to recharge the batteries for the fan, ND cookstoves may have an advantage for regions not on the grid.

One ND (Quad TLUD) and one FD (Philips) stove were investigated in this study. Both cookstoves are top-lit, which means that the biomass is initially ignited from the top and the high temperature layer propagates downwards through the packed bed. The top-ignition method produces significantly less PM, CO and NO_x compared to the bottom-ignition method with no significant difference in cookstove efficiency (Bhattacharya et al., 2002) and this might explain why the cookstove manufacturers recommend the top-ignition method. Convection is the major mode of heat transfer to the fuel during bottom-lit ignition, whereas conduction and radiation dominate the heat transfer for the top-lit ignition. In the top-lit ignition method, fuel is ignited at top and the heat is transferred to the fuel beneath through conduction. The packed bed can be divided into three zones starting from top to bottom: the gasification zone characterized by the highest temperature, the devolatilization zone and the drying zone.

The primary airflow is much lower than the secondary airflow due to the cookstove design and resistance of the packed bed. Oxygen deficiency, due to low primary airflow rate combined with high temperature in the primary oxidation zone, leads to the gasification of fuel generating producer gas consisting mainly of CO and N_2. The producer gas then mixes with the secondary air at the top of the stove producing a more stable and smokeless flame compared to traditional stoves. This process of transferring carbon from solid fuel to gaseous fuel (producer gas) followed by its combustion in a controlled sequential manner is what makes combustion in a gasification-based cookstove efficient. This modular function (primary and secondary oxidation zone) ensures flame generation at the top of the cookstove irrespective of the fuel level in the stove. Producer gas also contains tar, but in much lower concentrations compared to CO and N_2, which participates in particle formation if not oxidized completely in the secondary oxidation zone.

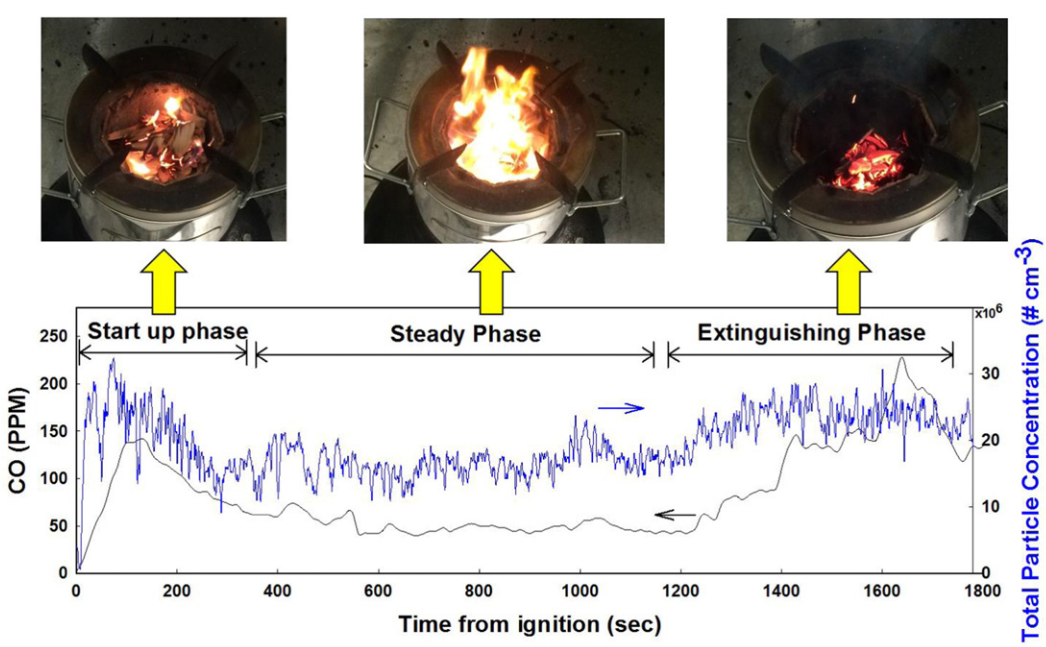

Fig. 3. Three combustion phases of the Philips stove fueled with applewood chips and corresponding real-time CO and total particle concentration profiles.

Table 2
Design parameters of the stoves.

	Philips	Quad TLUD
Height (cm)	30	43
Distance between primary and secondary air inlets (cm)	12	21.5
Diameter of inner cylinder (cm)	11.5	18
Diameter of outer cylinder (cm)	18.5	22.5
Fuel chamber capacity (cm^{-3})	1350	5468
Material of construction	Stainless steel	Sheet metal
Insulation	Ceramic inner walls	None

Since CO is intentionally produced in the primary oxidation zone, it is of utmost importance to oxidize it in the secondary oxidation zone to ensure the user's safety.

The primary and secondary airflow rates are key parameters to tune the performance of gasification-based cookstoves. Airflow rate can be controlled in FD cookstoves by adjusting the fan speed but the primary and secondary airflow rates cannot be controlled individually in most of the single fan models. Very few FD gasification-based cookstove models come with two separate fans to control both the primary and secondary airflow rate. The airflow control mechanism in ND stoves, if available, usually does not offer an airflow range as wide as in FD stoves and hardware modifications may be necessary. Too low secondary airflow rates result in incomplete oxidation of the gasification products in the secondary oxidation zone due to insufficient oxygen. Too high secondary airflow rates lower residence time of the producer gas in the secondary oxidation zone resulting in incomplete combustion. High flow rates also lower the temperature of the oxidation zone which decelerate the oxidation reactions.

Experiments were performed to study the effect of airflow rate on particulate emission characteristics of the Philips stove. The Philips stove fueled with applewood chips was tested at a high, medium and low airflow rate. The PNSD are presented in Fig. 4. The lowest particle number concentrations were observed for a medium airflow indicating that there is an optimum airflow which leads to the most efficient combustion. For this reason, the Philips cookstove was operated at a medium airflow setting for all further experiments. Previous modeling studies (Yang et al., 2004; Zhou et al., 2005) also reported an optimum airflow rate for maximum thermal efficiency and lowest gaseous emissions. A low airflow rate leads to incomplete combustion and a high airflow rate leads to heat loss because of excess air, thus decreasing the temperature of the oxidation zone.

Results and discussions

In this study, characterization of gaseous and PM emissions from two gasification-based improved cookstoves was performed. Three fuels: applewood, cowdung cake and coal were tested. Real-time measurements of PNSD, $PM_{2.5}$. lung-deposited surface area, CO, NO_x and CO_2 were collected and the average levels during steady-state phase are reported. Combustion efficiency was characterized by the CO–CO_2 ratio. Correlation tests were also performed on all pollutants and the CO–CO_2 ratio.

Particulate emissions

Tests 1 to 4 (Philips) and 5 to 8 (TLUD) are for comparison of emissions for different fuels. Fig. 5 presents PNSD measured for each cookstove for (A) coal and dung, (B) applewood chips and chunks, with corresponding values of particle geometric mean diameter (GMD), standard deviation and number concentration presented in Table 3. During the flame phase, coal produced higher concentrations (Philips: 2.42×10^9 # cm^{-3}, TLUD: 1.83×10^9 # cm^{-3}) of larger particles (Philips GMD: 221 nm, TLUD GMD: 255 nm) compared to the other fuels. In a field study, Zhang and Smith (2007) reported a much lower mean diameter (70.3–75.7 nm) for honeycomb briquette, made from a mixture of anthracite coal and clay, during first 15 min of combustion. This could be due to improved combustion as the honeycomb shape provides higher surface area and better airflow mixing through the cookstove. For both cookstoves, particle GMD during the coal smoldering phase (Philips: 84 nm, TLUD: 72 nm) was significantly lower than that of the coal flame phase. This could be attributed to a reduced devolatilization rate and thus lower tar production rate during the smoldering phase.

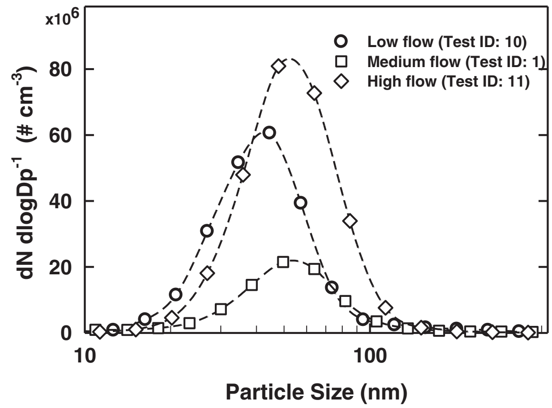

Fig. 4. Effect of airflow rate on particle number size distribution for the Philips stove fueled with applewood chips.

The second highest particle concentration and mean size was observed for dung cakes for both the Philips (number concentration: 1.17×10^9 # cm^{-3}, GMD: 112 nm) and the TLUD stove (number concentration: 6.84×10^8 # cm^{-3}, GMD: 85 nm). The difference between these two cookstoves can be explained by the higher airflow rate in the Philips cookstove compared to the TLUD stove. Tiwari et al. (2014)

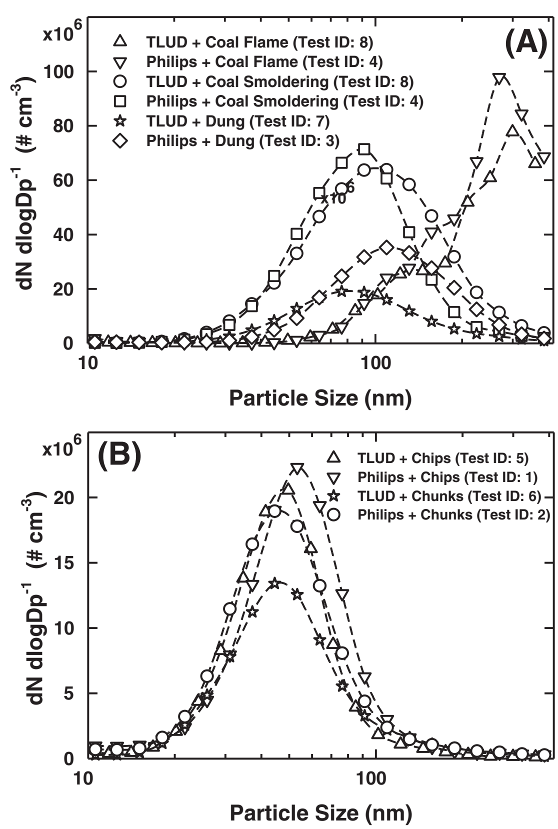

Fig. 5. Steady-state particle number size distribution for the TLUD and Philips stove with (A) coal and dung (B) applewood chips and chunks.

Table 3
Geometric mean diameter, standard deviation and total number of concentration during steady-state operation of the TLUD and Philips stove.

Test ID	Experiment	Geo. Mean Dia. (nm)	Geo. Std. Deviation	Total number Conc. (#/cc)
8	TLUD Coal Flame	255	1.51	1.83×10^9
4	Philips Coal Flame	221	1.64	2.42×10^9
8	TLUD Coal Smoldering	72	1.77	2.29×10^9
4	Philips Coal Smoldering	84	1.61	2.18×10^9
7	TLUD Dung	85	1.76	6.84×10^8
3	Philips Dung	112	1.66	1.17×10^9
5	TLUD Applewood Chips	46	1.56	5.20×10^8
1	Philips Applewood Chips	51	1.64	6.00×10^8
6	TLUD Applewood Chunks	49	1.70	3.99×10^8
2	Philips Applewood Chunks	48	1.67	5.56×10^8

reported much higher GMD for cowdung (152 nm) burned in a traditional U-shaped cookstove. Applewood, both chips and chunks, emitted smaller particles than dung and coal.

Fig. 6 displays bar charts of $PM_{2.5}$, mass concentration, lung-deposited surface area and total surface area concentration. There is no $PM_{2.5}$ and lung-deposited surface area data for any of the coal runs because the instruments were unable to measure such high concentrations. Therefore, mass concentrations (Fig. 6B) were also calculated from the PNSD data. As depicted in Fig. 5A, a significant fraction of particles generated during the smoldering phase of coal exceeded the detection limit and thus the calculated mass concentration values are an underestimation of actual levels. The most marked difference in $PM_{2.5}$ levels between cookstoves was for dung cakes. The Philips stove demonstrated a mean concentration of 119.80 mg m^{-3} compared to 9.08 mg m^{-3} for the TLUD stove. Although the Philips stove also demonstrated a higher $PM_{2.5}$ for applewood chips and chunks, the difference was less significant. It was observed during the experiments that the TLUD stove flame length was higher compared to the Philips stove with the same fuel type. Smaller flames, combined with higher secondary airflow in the Philips stove, reduced the residence time of gasification products in the secondary oxidation zone. Moreover, increasing differences between the $PM_{2.5}$ levels of the two stoves, operating with the same fuel, was observed with increasing fuel size (chips: 11.1%, chunks: 28.1%, dung: 1219.4%). The larger size of the dung cake resulted in the lowest packing efficiency, thus providing the lowest resistance for primary airflow which enhanced the effect of a higher flow rate on cookstove combustion efficiency. This observation highlights the issue of fuel compatibility for a given cookstove. Lung-deposited surface area (Fig. 6C) and total surface area concentrations (Fig. 6D) demonstrated similar trends to $PM_{2.5}$. However, lung-deposited surface area may be a better PM metric than $PM_{2.5}$ to understand health impacts of PM emissions characterized by high number concentration of smaller particles (Sahu et al., 2011).

Gaseous emissions

Fig. 7 presents data on NO_x, CO and $CO–CO_2$ ratio. The $CO–CO_2$ ratio (Li et al., 2009), i.e. the ratio of partially oxidized to fully oxidized

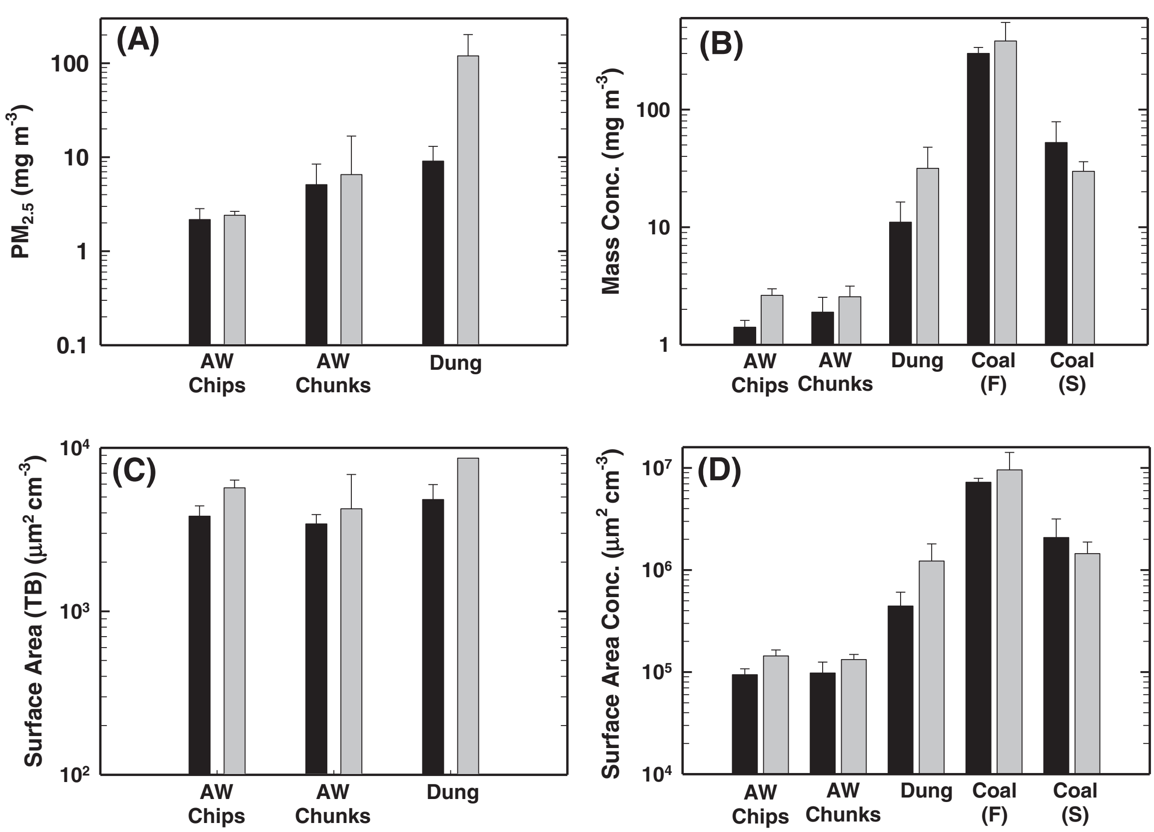

Fig. 6. Steady-state (A) $PM_{2.5}$, (B) mass concentration, (C) lung-deposited surface area and (D) surface area concentration for the TLUD stove (■) and the Philips stove (■).

carbon, may be a better proxy of combustion efficiency from the exposure perspective than the modified combustion efficiency (MCE), which is defined as $CO_2/(CO + CO_2)$ (Jetter et al., 2012). MCE is less sensitive to change in CO levels compared to the CO–CO_2 ratio on a molar basis.

NO_x formation rates depend on the temperature and the source of nitrogen which can either be from fuel or ambient air. In a typical packed bed biomass combustion system, nitrogen (N) from fuel is the main source of NO_x formation (Glarborg et al., 2003). Dung has the highest N content, followed by coal and applewood (Venkataraman & Rao, 2001; Glarborg et al., 2003; Roy et al., 2010; Winter et al., 1999). From Fig. 7A, it can be clearly observed that the N content of the fuel is not the only factor governing NO_x formation, as NO_x levels of applewood chips with the Phillips stove (47 ppm) are comparable to that of dung (59 ppm) whose N content is around six times higher than applewood. In addition, higher temperatures promote NO_x formation (Zhang & Smith, 2007; Skreiberg et al., 1997) which may explain the higher NO_x concentration measured for the Philips stove compared to the TLUD stove for applewood and coal. The Philips stove combustion chamber is lined with a layer of ceramic material which ensures low heat loss through the walls and thus higher temperatures. The similar level of NO_x observed during dung combustion for each of the stoves may be due to its significantly higher N content. In addition, the lower NO_x levels observed from coal during the flame phase, as compared to the smoldering phase, for both stoves could be due to lower temperatures during the flame phase because of highly endothermic devolatilization reactions and moisture evaporation from the unburned coal.

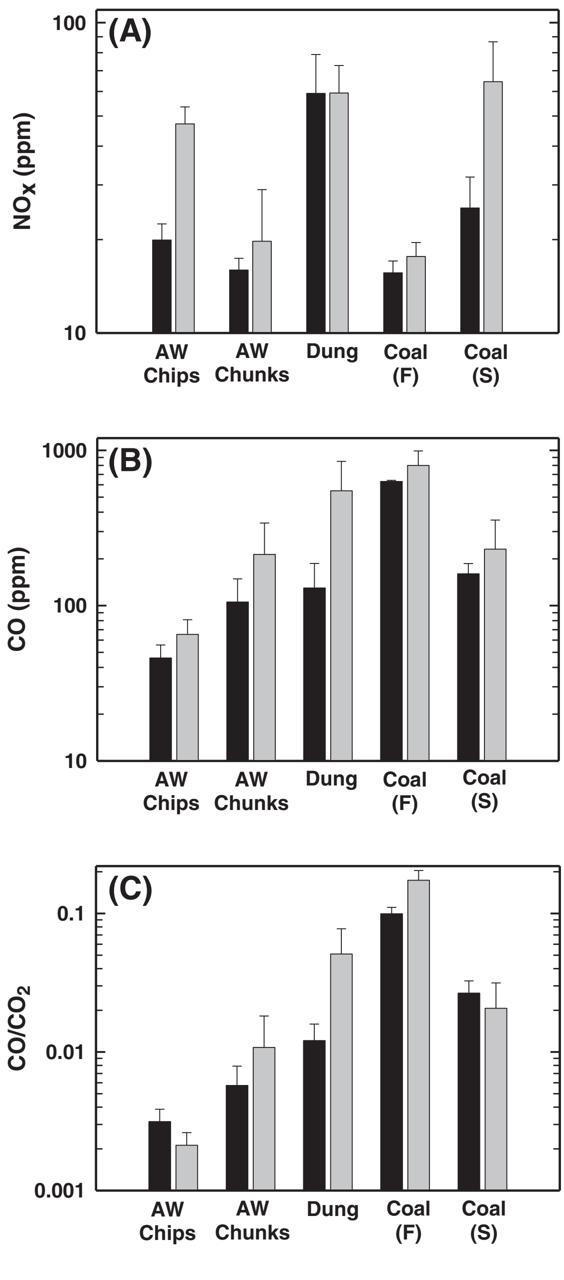

Fig. 7. Steady-state concentrations of (A) NO_x, (B) CO and (C) CO–CO_2 ratio for the TLUD stove (■) and the Philips stove (■).

CO is the major product from biomass gasification in the primary oxidation zone. A gasification-based stove must efficiently oxidize it to CO_2 in the secondary oxidation zone. As demonstrated in Fig. 7B, significantly higher CO levels were observed with the Philips stove fueled with coal during the flame phase (800 ppm) and dung cakes (548 ppm), and the TLUD stove fueled with coal during the flame phase (632 ppm). Though these concentrations were measured in the plume, burning coal or dung cakes in similar stoves in a poorly ventilated setting may lead to subtle cardiovascular and neurobehavioral effects at low level chronic concentrations and even death at acute concentrations of CO (Raub et al., 2000). The TLUD stove had lower CO concentrations than the Philips stove for all fuels, especially dung (Philips: 548 ppm, TLUD: 130 ppm). The CO concentration trends were similar to the PM concentration, thus the same explanation that more gasification products remain unoxidized in the Philips stove due to the lower residence time in the secondary oxidation zone, may be given. A more detailed discussion on the correlations between these metrics is provided in the next section.

To investigate the effect of fuel size on concentrations of gaseous pollutants, two different sizes of applewood (chips and chunks) were tested. CO levels decreased with decreasing fuel size (Philips: 213 ppm (chunks) and 65 ppm (chips), TLUD: 106 ppm (chunks) and 46 ppm (chips)) while NO_x showed the opposite trend (Philips: 20 ppm (chunks) and 47 ppm (chips), TLUD: 16 ppm (chunks) and 20 ppm (chips)). Similar trends have been reported by Bhattacharya et al. (2002) who suggested that the smaller size of the fuel intensified combustion thus promoting higher temperatures, facilitating CO oxidation and NO_x formation.

Correlation tests between different pollutants

Correlations between concentrations of different pollutants can be explored to see whether one pollutant may be used as a proxy for another. The primary focus was to investigate correlations between gaseous and particulate emission parameters. Table 4 presents a correlation coefficient (r) matrix with p-values for the 95% confidence interval. No significant correlations were observed between NO_x and the PM metrics at the 95% confidence interval, with the exception of lung-deposited surface area ($r = 0.455$). Strong correlations between PM metrics and CO levels were expected, as both are products of incomplete combustion. However, CO demonstrated only moderate positive correlations with particle GMD ($r = 0.702$), surface area concentration ($r = 0.646$) and mass concentration ($r = 0.645$). Also, weak correlations between CO and lung-deposited surface area ($r = 0.445$) and total number concentration ($r = 0.394$) were also observed. A moderately strong correlation ($r = 0.760$) was observed between CO and $PM_{2.5}$ which is similar to correlations reported in the literature by Venkataraman & Rao (2001) ($R^2 = 0.71$). Likewise in a field study, Chowdhury et al. (2012) reported correlations (R^2) between $PM_{2.5}$ and CO concentrations ranging from 0.605 to 0.705 depending upon the type of cookstove. In a similar study, Commodore et al. (2013) correlated 4-h mean personal $PM_{2.5}$ exposures with personal CO exposures during lunch ($r = 0.67$) and dinner ($r = 0.72$). Leavey et al. (2015) reported an r-value of 0.71 for the correlation between average $PM_{2.5}$ and CO concentrations over the steady-state phase.

Table 4
Correlation coefficient (r) matrix with p-values, corresponding to 95% confidence interval, in parentheses.

	CO/CO_2	CO	CO_2	NO_x	LDSA	$PM_{2.5}$	TNC	GMD	SA Conc.
CO/CO_2									
CO	0.883 (<0.001)								
CO_2	-0.615 (<0.001)	-0.535 (<0.001)							
NO_x	-0.278 (0.086)	-0.201 (0.21)	0.181 (0.25)						
LDSA	0.496 (0.022)	0.445 (0.038)	0.010 (0.967)	0.455 (0.033)					
$PM_{2.5}$	0.857 (<0.001)	0.760 (<0.001)	-0.453 (0.020)	0.289 (0.152)	0.625 (0.001)				
TNC	0.613 (<0.001)	0.394 (0.023)	-0.597 (<0.001)	0.001 (0.99)	0.750 (<0.001)	0.943 (<0.001)			
GMD	0.900 (<0.001)	0.702 (<0.001)	-0.541 (<0.001)	0.039 (0.82)	0.568 (0.014)	0.835 (<0.001)	0.556 (<0.001)		
SA Conc.	0.908 (<0.001)	0.646 (<0.001)	-0.510 (0.002)	-0.105 (0.560)	0.681 (0.002)	0.941 (<0.001)	0.712 (<0.001)	0.902 (<0.001)	
Mass Conc.	0.905 (<0.001)	0.645 (<0.001)	-0.464 (0.006)	-0.113 (0.530)	0.641 (0.004)	0.929 (<0.001)	0.636 (<0.001)	0.909 (<0.001)	0.993 (<0.001)

LDSA Lung Deposited Surface Area
TNC Total Number Concentration
GMD Geometric Mean Diameter
SA Conc. Surface Area Concentration
Mass Conc. Mass Concentration

Even weaker correlations were observed between the PM metrics and CO_2, with the exception of total number concentration. This indicates that PM emissions are not only dependent on the combustion rate, but also on the extent of combustion. To demonstrate this, correlation tests were performed between $CO–CO_2$ ratios and PM metrics. Stronger correlations of $PM_{2.5}$ ($r = 0.857$), particle GMD ($r = 0.900$), surface area concentration ($r = 0.908$) and mass concentration ($r = 0.905$) with $CO–CO_2$ ratio (Fig. 8) were observed. This suggests that CO concentration normalized by an indicator of combustion rate (CO_2 in this study) is a better proxy for PM metrics than CO alone. Moderate correlation ($r = 0.625$) was found between $PM_{2.5}$ and lung-deposited surface area. Leavey et al. (2015) reported a similar correlation ($r = 0.64$) between $PM_{2.5}$ and lung-deposited surface area during steady-state. This highlights the possibility of translating the correlations between different pollutants from laboratory to field and vice versa. The $CO–CO_2$ ratio demonstrated a weaker correlation with lung-deposited surface area ($r = 0.496$) compared to total surface area concentration calculated from PNSD ($r = 0.908$) as the two surface area concentrations are interrelated by a deposition efficiency curve which is not linear.

Insignificant correlations between NO_x and CO, CO_2 and $CO–CO_2$ ratio were observed. Mass concentration, surface area concentration and GMD demonstrated a high correlation ($r > 0.835$) with each other. Likewise, a strong correlation ($r = 0.929$) was observed between $PM_{2.5}$ and mass concentration calculated from PNSD data because only a small fraction of particles was observed around the upper detection limit of SMPS for all fuels except coal flame phase. The total number concentration demonstrated a moderate correlation with particle GMD ($r = 0.556$), mass concentration ($r = 0.636$) and surface area concentration ($r = 0.712$).

Effect of a cooking pot on emission characteristics

The TLUD cookstove fueled with applewood chips was tested with and without a cooking pot. As presented in Fig. 9A, increased concentrations were observed for CO, $PM_{2.5}$ and lung-deposited surface area when a pot was used, but the opposite trend was observed for NO_x. Concentration of CO was almost 10 times higher when a pot was added. This may be due to changes in the flame structure and obstruction of airflow caused by the physical presence of the cooking pot. Also, the addition of

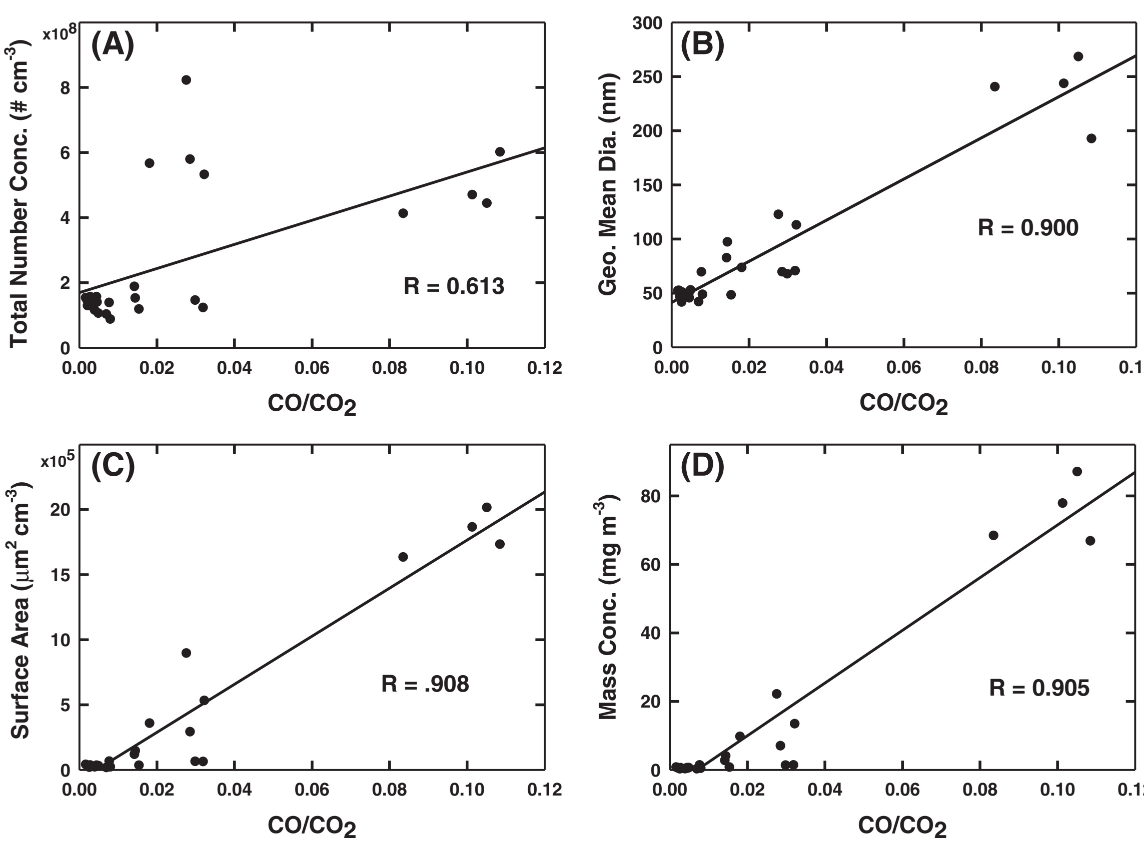

Fig. 8. Correlations between $CO–CO_2$ ratio and (A) total number concentration, (B) geometric mean diameter, (C) surface area concentration and (D) mass concentration.

a pot may lower the gasification zone temperature which reduces the rate of NO_x formation and rate of oxidation of CO and VOCs. $PM_{2.5}$ also increased by a factor of 10 from 2.16 mg m^{-3} to 21.4 mg m^{-3} with the addition of a pot, demonstrating a similar trend as CO. However, a relatively smaller difference was observed for lung-deposited surface area (with pot: 4256 μm^2 cm^{-3}, without pot: 3816 μm^2 cm^{-3}). This indicates that the addition of a cooking pot promoted the formation of larger particles, for example in Fig. 8B, particle GMDs were 69 nm (with pot) and 46 nm (without pot), whereas no significant change was observed for the total number concentration (5.40×10^8 # cm^{-3} with pot and 5.20×10^8 # cm^{-3} without pot). The addition of a pot changes multiple factors such as flame temperature and structure, and airflow characteristics. Therefore, it is hard to associate the observed changes in pollutant characteristics to a single cause. This highlights the importance of studying these cookstoves without a pot but understanding the effect of pot is also critical as it reflects the real field conditions.

Conclusions

This study compared the gaseous and particulate pollutant characteristics from two gasification-based improved cookstoves fed with different types of fuel. Pollutant concentrations from coal and dung combustion were significantly higher than that of applewood. The ND TLUD stove demonstrated lower PM concentration compared to the FD Philips stove which could be attributed to a higher airflow rate and lower height of the Philips stove. Moreover, differences in $PM_{2.5}$ levels between the two stoves, operated with the same fuel, increased with increasing fuel size. The trends observed in pollutant concentrations were explained by the design and operating principle of gasification-based cookstoves. Fuel choice is governed by multiple factors such as household income, season and geographical location which leads to fuel stacking. Both cookstoves studied demonstrated significant difference in the emission levels with different types of fuel. Therefore, it is important for an improved cookstove to be compatible with multiple fuels common in the target region to achieve desired health and environmental impacts. High concentrations of pollutants were observed for dung cakes and coal indicating that section of the population lying at the bottom of energy ladder is at a greater risk. Therefore, it is tentatively suggested that a cookstove should be designed specifically for dung cake and coal.

Strong correlations between $CO–CO_2$ ratio and $PM_{2.5}$, particle GMD and surface area concentration were observed. Thus, $CO–CO_2$ ratio may be used as a proxy for the particulate metrics. The $CO–CO_2$ ratio is an indicator of combustion efficiency, a higher ratio indicative of a lower efficiency. Since PM is also a product of incomplete combustion, the two metrics correlate well. It is important to note, however, that any such quantitative correlation factor may not be applicable with other types of cookstove, fuel, or experimental design. The presence of a pot could also affect the nature of such correlations.

Combustion in cookstoves is a complex process. This study demonstrated the importance of operating parameters and cookstove design in reducing the pollutant concentrations. More attention should be given to developing detailed cookstove combustion models that enhance the understanding between cookstove design, operation and performance to facilitate the engineering of the next generation of improved cookstoves. Though significantly cleaner than traditional cookstoves, improved cookstoves still emit high concentrations of pollutants. Therefore, they should be viewed only as an interim solution towards the goal of providing cleaner energy for household use.

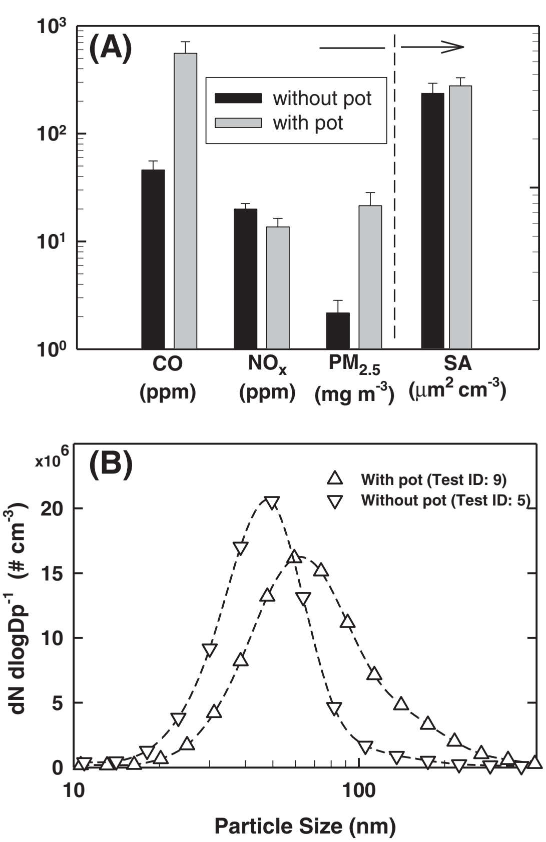

Fig. 9. Effect of a cooking pot on (A) concentrations of CO, NO_x, $PM_{2.5}$ and lung-deposited surface area (SA) and (B) PNSD from the TLUD stove fueled with applewood chips.

Acknowledgements

This work was partially supported by the McDonnell Academy Global Energy and Environment Partnership (MAGEEP) of Washington University in St. Louis and a grant from the National Science Foundation (NSF CBET 1437933). SP thanks the McDonnell International Scholars Academy of Washington University in St. Louis and Arch Coal Inc. for the fellowship. The authors thank Smit Shah, IIT Gandhinagar, for help with experiments during a MAGEEP Summer Internship program.

References

Ahn K, Jung C, Choi M, Lee J. Particle sampling and real time size distribution measurement in H_2/O_2/TEOS diffusion flame. J Nanopart Res 2001;3(2-3):161–70.

Anon. Environment, Health, and Climate Change: A New Look at an Old Problem. Washington, DC: The World Bank; 2011.

Armendáriz-Arnez C, Edwards RD, Johnson M, Rosas IA, Espinosa F, Masera OR. Indoor particle size distributions in homes with open fires and improved Patsari cook stoves. Atmos Environ 2010;44(24):2881–6.

Arora P, Jain S, Sachdeva K. Laboratory based assessment of cookstove performance using energy and emission parameters for North Indian cooking cycle. Biomass Bioenergy 2014;69:211–21.

Bailey M. The new ICRP model for the respiratory tract. Radiat Prot Dosimetry 1994;53(1-4):107–14.

Bhattacharya SC, Albina DO, Myint Khaing A. Effects of selected parameters on performance and emission of biomass-fired cookstoves. Biomass Bioenergy 2002;23(5): 387–95.

Biswas P. Measurement of high concentration and high temperature aerosols. Aerosol Measurement: Principles, Techniques, and Applications; 2001. p. 2.

Bond TC, Covert DS, Kramlich JC, Larson TV, Charlson RJ. Primary particle emissions from residential coal burning: optical properties and size distributions. J Geophys Res Atmos 2002;**107**(D21). (1984–2012). (ICC 9-1–ICC 9-14).

Bruce N, Perez-Padilla R, Albalak R. Indoor air pollution in developing countries: a major environmental and public health challenge. Bull World Health Organ 2000;78(9): 1078–92.

Chengappa C, Edwards R, Bajpai R, Shields KN, Smith KR. Impact of improved cookstoves on indoor air quality in the Bundelkhand region in India. Energy Sustain Dev 2007; 11(2):33–44.

Chowdhury Z, Le LT, Masud A, Chang KC, Alauddin M, Hossain M, et al. Quantification of indoor air pollution from using cookstoves and estimation of its health effects on adult women in northwest Bangladesh. Aerosol Air Qual Res 2012;12(4):463–75.

Commodore AA, Hartinger SM, Lanata CF, Mäusezahl D, Gil AI, Hall DB, et al. A pilot study characterizing real time exposures to particulate matter and carbon monoxide from cookstove related woodsmoke in rural Peru. Atmos Environ 2013;79:380–4.

Erkman S, Ramaswamy R. Applied Industrial Ecology: A New Platform for Planning Sustainable Societies: Focus on Developing Countries with Case Studies from India. Aicra Publishers; 2003.

Fang J, Leavey A, Biswas P. Controlled studies on aerosol formation during biomass pyrolysis in a flat flame reactor. Fuel 2014;116:350–7.

Glarborg P, Jensen AD, Johnsson JE. Fuel nitrogen conversion in solid fuel fired systems. Prog Energy Combust Sci 2003;29(2):89–113.

Global Health Observatory. World Health Organization available from: http://www.who.int/gho/en/ (accessed 7 April 2014).

Jetter JJ, Kariher P. Solid-fuel household cook stoves: characterization of performance and emissions. Biomass Bioenergy 2009;33(2):294–305.

Jetter J, Zhao Y, Smith KR, Khan B, Yelverton T, DeCarlo P, et al. Pollutant emissions and energy efficiency under controlled conditions for household biomass cookstoves and implications for metrics useful in setting international test standards. Environ Sci Technol 2012;46(19):10827–34.

Just B, Rogak S, Kandlikar M. Characterization of ultrafine particulate matter from traditional and improved biomass cookstoves. Environ Sci Technol 2013;47(7):3506–12.

Kandpal J, Maheshwari R. Combustion of biomass fuels in two cookstoves for their conservation. Energy Convers Manag 1995;36(10):1015–21.

Kar A, Rehman IH, Burney J, Puppala SP, Suresh R, Singh L, et al. Real-time assessment of black carbon pollution in Indian households due to traditional and improved biomass cookstoves. Environ Sci Technol 2012;46(5):2993–3000.

Leavey A, Fang J, Sahu M, Biswas P. Comparison of measured particle lung-deposited surface area concentrations by an Aerotrak 9000 using size distribution measurements for a range of combustion aerosols. Aerosol Sci Tech 2013;47(9):966–78.

Leavey A, Londeree J, Priyadarshini P, Puppala J, Schechtman KB, Yadama G, et al. Real-time particulate and CO concentrations from cookstoves in rural households in Udaipur, India. Environ Sci Technol 2015.

Legros G. The Energy Access Situation in Developing Countries: A Review Focusing on the Least Developed Countries and Sub-Saharan Africa. New York: World Health Organization and United Nations Development Program; 2009.

Li X, Wang S, Duan L, Hao J, Nie Y. Carbonaceous aerosol emissions from household biofuel combustion in China. Environ Sci Technol 2009;43(15):6076–81.

L'Orange C, Volckens J, DeFoort M. Influence of stove type and cooking pot temperature on particulate matter emissions from biomass cook stoves. Energy Sustain Dev 2012;16(4):448–55.

MacCarty N, Ogle D, Still D, Bond T, Roden C. A laboratory comparison of the global warming impact of five major types of biomass cooking stoves. Energy Sustain Dev 2008;12(2):56–65.

MacCarty N, Still D, Ogle D. Fuel use and emissions performance of fifty cooking stoves in the laboratory and related benchmarks of performance. Energy Sustain Dev 2010;14(3):161–71.

McKendry P. Energy production from biomass (part 1): overview of biomass. Bioresour Technol 2002;83(1):37–46.

Naeher LP, Brauer M, Lipsett M, Zelikoff JT, Simpson CD, Koenig JQ, et al. Woodsmoke health effects: a review. Inhal Toxicol 2007;19(1):67–106.

Pohekar SD, Kumar D, Ramachandran M. Dissemination of cooking energy alternatives in India—a review. Renew Sustain Energy Rev 2005;9(4):379–93.

Raub JA, Mathieu-Nolf M, Hampson NB, Thom SR. Carbon monoxide poisoning—a public health perspective. Toxicology 2000;145(1):1–14.

Rehfuess E. Fuel for life: household energy and health. World Health Organization; 2006.

Roden CA, Bond TC, Conway S, Pinel ABO. Emission factors and real-time optical properties of particles emitted from traditional wood burning cookstoves. Environ Sci Technol 2006;40(21):6750–7.

Roy PC, Datta A, Chakraborty N. Assessment of cow dung as a supplementary fuel in a downdraft biomass gasifier. Renew Energy 2010;35(2):379–86.

Sahu M, Peipert J, Singhal V, Yadama GN, Biswas P. Evaluation of mass and surface area concentration of particle emissions and development of emissions indices for cookstoves in rural India. Environ Sci Technol 2011;45(6):2428–34.

Shen G, Wang W, Yang Y, Ding J, Xue M, Min Y, et al. Emissions of PAHs from indoor crop residue burning in a typical rural stove: emission factors, size distributions, and gas−particle partitioning. Environ Sci Technol 2011;45(4):1206–12.

Singh D, Gadi R, Mandal T, Saud T, Saxena M, Sharma S. Emissions estimates of PAH from biomass fuels used in rural sector of Indo-Gangetic Plains of India. Atmos Environ 2013;68:120–6.

Skreiberg Ø, Glarborg P, Jensen A, Dam-Johansen K. Kinetic NO_x modelling and experimental results from single wood particle combustion. Fuel 1997;76(7):671–82.

Smith KR. Indoor air pollution in developing countries: recommendations for research†. Indoor Air 2002;12(3):198–207.

Tiwari M, Kumar Sahu S, Chindhu Bhangare R, Yousaf A, Girish Pandit G. Particle size distributions of ultrafine combustion aerosols generated from household fuels. Atmos Pollut Res 2014;5(1).

Venkataraman C, Rao GUM. Emission factors of carbon monoxide and size-resolved aerosols from biofuel combustion. Environ Sci Technol 2001;35(10):2100–7.

Verma VK, Bram S, Delattin F, Laha P, Vandendael I, Hubin A, et al. Agro-pellets for domestic heating boilers: standard laboratory and real life performance. Appl Energy 2012;90(1):17–23.

Water Boiling Test Protocol. Global Alliance for Clean Cookstoves. http://cleancookstoves.org/binary-data/DOCUMENT/file/000/000/399-1.pdf (Accessed on 20 Nov 2015).

Winter F, Wartha C, Hofbauer H. NO and N_2O formation during the combustion of wood, straw, malt waste and peat. Bioresour Technol 1999;70(1):39–49.

Yang YB, Sharifi VN, Swithenbank J. Effect of air flow rate and fuel moisture on the burning behaviours of biomass and simulated municipal solid wastes in packed beds. Fuel 2004;83(11–12):1553–62.

Yang D, Zhang XJ, Chen QW, Zhang M, Wei SJ. Experimental study on NO reduction by biomass reburning in Northern China. Green Building, Materials and Civil Engineering; 2014. p. 239.

Zhang J, Smith KR. Household air pollution from coal and biomass fuels in China: measurements, health impacts, and interventions. Environ Health Perspect 2007;115(6):848–55.

Zhang H, Wang S, Hao J, Wan L, Jiang J, Zhang M, et al. Chemical and size characterization of particles emitted from the burning of coal and wood in rural households in Guizhou, China. Atmos Environ 2012;51(0):94–9.

Zhou H, Jensen AD, Glarborg P, Jensen PA, Kavaliauskas A. Numerical modeling of straw combustion in a fixed bed. Fuel 2005;84(4):389–403.